9B.4 POLARIMETRIC WEATHER RADAR CALIBRATION - ENGINEERING CHALLENGES

Richard L. Ice* and J. G. Cunningham
U.S. Air Force, Air Weather Agency, Operating Location K, Norman, Oklahoma
A. K. Heck, WSR-88D Radar Operations Center, Norman, Oklahoma

1. INTRODUCTION

The deployment of the polarimetric upgrade to the United States' Next Generation Doppler weather radar network (NEXRAD) is nearly complete. The program only has a few remaining WSR-88D radars to retrofit, and these are located overseas. The network within the CONUS is now fully polarimetric.

Accurate calibration of the new hardware is essential for the NEXRAD community to gain maximum benefit from use of the new polarimetric variables. The most critical parameter is differential reflectivity (Zdr), which is derived from the ratio of return powers in the horizontal and vertical channels. In order to retrieve the intrinsic, or true, measure of Zdr, the contribution of the radar hardware itself to this power ratio must be removed. This contribution, or bias, originates from several components of the radar. There can be an imbalance in the transmitted powers, i.e. the horizontal and vertical components of the divided transmitter power may not be equal. The gains of the antenna in the horizontal and vertical paths may not be exactly the same, and finally, the two receiver channels will likely not exhibit the same overall gain and will generate different levels of electronic noise.

Accurately determining the biases related to the horizontal and vertical channels in all these subsystems constitutes the process of differential reflectivity calibration. This paper reviews the Zdr calibration methods provided in the initial design and development of the upgrade and provides descriptions and status of development for the current projects underway at the WSR-88D Radar Operations Center (ROC), the National Center for Atmospheric Research (NCAR) and the National Severe Storms Laboratory (NSSL). These partners are actively pursuing new methods of monitoring the state of Zdr calibration in the network, and are developing modifications to the calibration process in order to provide the necessary accuracy. In particular, the ROC and NCAR are implementing an external method based on the use of cross polarization power returned from ground clutter (Hubbert, 2003).

This paper reviews the challenges of both implementing this new technique in the WSR-88D and maintaining the calibration state using the current methods.

2. MOTIVATION – WHY CALIBRATE?

Prior to the polarimetric upgrade, precipitation estimation algorithms were primarily based on reflectivity. The traditional requirement for the uncertainty in the reflectivity estimate (dBz, Smith, 2010) is 1.0 dBz (Sirmans, 1992, Ice, 2005). This is the level of accuracy needed to obtain acceptable rainfall rate accuracy. While the original WSR-88D hardware and software was believed to be capable of calibration to this requirement, it proved difficult to achieve in practice in the early days of NEXRAD (Ice, 2005). In fact, upon the initial deployment of the network in the early 1990's, the government did not have a viable method for calibrating the hardware.

The Operational Support Facility (OSF) Engineering Branch developed a comprehensive method for reflectivity calibration, but problems remained until a network monitoring capability was established. This capability was based on a software tool that compared the reflectivities from adjacent radars with the objective of identifying specific units that required attention when their estimates on common volumes of precipitation were in disagreement with their neighbors (Gourley, 2003). Reflectivity calibration accuracy and stability was not consistently achieved until this monitoring capability was in place and several issues with antenna gain measurement were resolved (Ice, 2005).

With the polarimetric capability, a new Qualitative Precipitation Estimation (QPE) algorithm is being deployed (Berkowitz, 2013). This algorithm relies on the new polarimetric variables in order to provide precipitation estimates with less error

* Corresponding Author Address: Richard L. Ice, US Air Force., WSR-88D Radar Operations Center, 1313 Halley Circle. Norman, OK, 73069

e-mail: Richard.L.Ice@noaa.gov

The views expressed are those of the authors and do not necessarily represent those of the United States Air Force.

than the legacy algorithm which used reflectivity alone. The QPE method consists of three parts: (1) Hydrometeor Detection Algorithm (HCA), (2) Melting Layer Detection Algorithm (MLDA), and (3) the QPE algorithm itself. The outputs of the HCA and MLDA are critical inputs to the QPE. All three use reflectivity, differential reflectivity, cross correlation coefficient, and specific differential phase as inputs.

In order for the QPE to perform substantially better than the legacy estimator, the differential reflectivity must be estimated to within an error limit of 0.1 to 0.2 dB (Ryzhkov, 2005). For light to moderate rain, the 0.1 dB accuracy must be achieved to maintain rain rate error estimates to around 10 %. For heavier rain, the accuracy can be relaxed to 0.2 dB. If the error in calibration is greater than about 0.3 dB, then the polarimetric precipitation estimators do not perform substantially better than the legacy algorithm.

The primary source of error in the Zdr estimate is the uncertainty in the measurement of the system bias, or the contribution to the overall power ratio coming from the radar hardware. The accurate measurement of this value, the system bias, has been the focus of much attention over the past ten years (Zrnic, 2006).

Various methods for determining the system bias have been studied and used in the research community. The common practice is to obtain careful measurements of the differences between the two polarization channels (H and V) for the transmitter, receiver, and antenna performance. Even with careful measurements using well calibrated instruments however, the overall uncertainty of the bias has historically been greater than the required tolerance. Most research radars have been calibrated using a method that relies on the radar antenna being rotated through 360 degrees while being pointed in a vertical position in the presence of light precipitation (Gorgucci, 1999). Because the theory assumes that light precipitation falling towards the antenna is spherical, the mean Zdr in the resolution volume should be zero. Any mean value of the Zdr estimate obtained in this manner would be the value of the radar system bias.

The vertical pointing method has to date been considered the only reliable external means of obtaining the system bias. During the development of the prototype upgrade for NEXRAD, the KOUN radar was calibrated using careful engineering measurements (Zrnic, 2006). The program did not develop an external method although the use of precipitation at angles other than vertical were explored (Rhyzkkov, 2005).

3. THE WSR-88D BASELINE METHOD

The WSR-88D in its baseline configuration does not have the capability point vertically, so the classic method was not available for the production NEXRAD polarimetric upgrade without modifications to the antenna pedestal hardware. Also, it was deemed impractical to take the radars offline during precipitation events in order to perform calibration vertical pointing scans. Much of the focus of the design and development of the production hardware focused on calibration and the contractor, Baron Services Inc., provided the necessary hardware components and procedures for conducting what came to be known as an “engineering method”. This method is currently employed to obtain the bias components for the transmitted signal, the receiver channels, and the antenna.

Figure 1 is a simplified block diagram of the WSR-88D showing the three major subsytems relevant to Zdr calibration (transmitter, receiver, antenna). Note that the three subsystems come together at a common point known as the calibration reference plane. This is established as the dividing point for separating out the three distinct components of the overall system bias. At this point, waveguide couplers are provided that allow insertion of test signals (for receiver bias measurements) and for extracting samples of the signals within the waveguide (for transmitter power measurements).

The baseline hardware suite contains all of the necessary components for generating the receiver test signals and for extracting and processing the transmitter power samples from both channels. However, the monitoring hardware itself introduces biases, and these must be measured. Calibration is then the process of measuring the bias introduced by the receiver test signals (test signal bias) and the transmitter power measurement hardware (power sense bias), and the antenna bias (from solar scans).

3.1 Antenna Bias Measurement

The antenna bias is obtained from a relatively straightforward scan of the sun, relying on the assumption that the sun is un-polarized (Figure 2). This “sun bias” obtained from the scan is the ratio of noise powers between the two channels where the signal source is the noise power of the sun itself. However, the actual bias contribution from the antenna component can only be inferred from the results of the solar scan because the ratio of the noise powers obtained at the signal processor includes not only the bias from the antenna, but contains the bias from the receiver, and this must be removed. In the calibration system, the result of subtracting the receiver

bias from the sun bias measurement is called "reflector bias". Obviously, an error in measuring the receiver bias creates an error in the reflector bias.

3.2 Receiver Bias Measurement

The receiver bias measurement is demonstrated in Figure 3, which shows a simplification of the use of the test signal. Equal power continuous wave (CW) signals from the built-in test equipment (BITE) are inserted into the front end of the receiver channels using the couplers at the calibration reference plane. The desired outcome is that the test signals are equal in power and thus any non-zero ratio of powers obtained at the signal processor would be the result of the bias, or imbalance, between the H and V receiver. In reality, the powers in the two test signals are not exactly equal, and the total path losses from the BITE equipment to the inputs to the receivers are not equal. These differences, or the test signal bias, must be measured in an off line process completed at the time of calibration. The test signal bias is indicated by the red arrow in Figure 3. The test signal bias measurement is then stored in system adaptation data and used to adjust the periodic on-line receiver bias measurements.

3.3 Transmitter Bias Measurement

In an ideal radar, the transmitted H and V powers would always be equal. This could be achieved in practice by using a perfect splitter to divide the transmitter signal in to equal parts, and then by carefully matching the waveguide and circulator systems up to the antenna. In the case of the WSR-88D polarimetric upgrade, a more complex method of dividing the transmitter power is employed. The contractor delivered a capability to establish any ratio of transmitted power between the H and V channels through use of a variable phase power divider. This divider can continuously deliver ratios of H to V power under computer control ranging from all H to all V and any ratio in between. In normal operations, the power ratio is set such that the H and V transmitter powers are equal. Because the ratio is variable, and since it is never possible to perfectly match components, the H and V powers must be measured.

The transmitter power imbalance is measured in a similar manner, using the couplers at the calibration reference plane and the BITE system. Figure 4 illustrates the process. A unique feature of the transmitter power measurement is that the measurement device is the receiver signal processor itself, in particular the H receiver channel. The V and H powers have to be measured separately due to this and the fact that there is only one hardware delay line available in the BITE system. The sampled transmitter signals must be delayed because the receivers are blanked by the TR Limiter component during transmission. The BITE system provides the necessary switching and routing components for alternatively connecting the H and V couplers and routing the samples to the H receiver.

The BITE system introduces an error into the measurement of the ratio of the H and V samples, and this must be measured at the time of calibration. The power sense bias component is indicated by a function in Figure 4. Again, the power sense bias is stored in adaptation data and used to correct the power measurements when they are made periodically during operations.

3.4 Obtaining the Test Signal and Power Sense Bias Parameters

The biases from the test signal and power sense functions are obtained off-line when the technicians perform calibration. These biases are measured during a process where the technician crosses the connections to the calibration reference plane couplers, then runs automatic tests that record the output of the H channel receiver for both receiver bias tests and the transmitter power monitoring. Then the technicians return the coupler connections to the normal (uncrossed, or "straight") configuration and run the tests again. Figure 5 illustrates the process for the test signal bias. As seen in the diagram and accompanying equations, the difference in the H receiver outputs between the crossed and straight configurations yields the bias between the H and V test signals that exists at the input to the receiver.

This is a theoretically simple and elegant method for obtaining the test bias numbers. However, in practice, results of this process can be inconsistent. For this reason, the system procedures require that several measurements be made and a consistency check is done before final results are accepted.

The polarimetric hardware is mounted on the elevation arms of the antenna pedestal assembly. The advantage of this configuration is that the low noise amplifiers are located very near the antenna port, thus improving sensitivity. Also, since the power divider function is on the antenna, the H and V waveguide paths to the feed assembly are shortened, thus reducing effects of differing path lengths on overall system initial phase and perhaps allowing the system phase to be more stable over time. The disadvantage to this configuration is that maintenance can be difficult.

In order to perform the crossed and straight calibration process, the technicians must stand on a ladder and reach behind some of the waveguide components. Figure 6 shows a view of the RF microwave components, or the RF Pallet from the floor of the dome area with the ladder in place. The small inset photos of Figure 6 show the connectors and Heliax cables that are crossed for the tests. The connectors are of a snap-on variety that were selected to allow consistent results from multiple connections.

3.5 Continuous Calibration Process

During operations, the system Zdr is constantly measured and updated using the three calibration parameters discussed here. At the end of every volume scan, the BITE injects test signals into the receiver channels in order to update the receiver bias component of the overall system bias. The BITE also measures the noise power in each channel using a local noise source calibrated to a traceable standard. Periodically, typically every eight hours, the transmitter power balance is updated. The transmitter power ratio is not measured every volume because the process takes about 2 minutes and this would cause unacceptable delays in the volume update rate. The antenna bias measurement is done less frequently, on a monthly scale.

4. OBSERVED SYSTEM PERFORMANCE

The development teams and the government spent considerable effort reviewing, analyzing, and testing the hardware and software systems with respect to calibration. However, due to the challenging nature of verifying the Zdr bias externally, there was no formal test of the calibration capability. The contractor was required to verify compliance with the 0.1 dB accuracy specification by use of analysis. Baron Services engineers conducted a theoretical analysis which included some hardware measurements. This analysis demonstrated that the delivered design was capable of meeting the requirement (Baron Services, 2011) and the government accepted the results (Saxion, 2012).

Engineers at Baron, working with data obtained shortly after initial installations, analyzed the Zdr bias measurements and concluded that the system was performing as designed (Balaji, 2012). Figure 7, from Balaji, shows the system bias values for ten radars obtained every volume for 1600 trials. The histograms and time series plots show the stability of the process was quite good, although there is a range of Zdr values between the sites. One site exhibited a system bias of less than -1.3, which was greater than the average of the other sites and could indicate an error in calibration.

ROC engineers and the joint Data Quality Team also monitored the hardware performance on a regular basis, during both the development as well as the early deployment stages (Saxion, 2012). Initial results were encouraging, showing very good stability in the hardware over time and early indications were that the test radar calibration was adequate, as well as it could be assessed with the emerging external verification methods. These methods were based on observing expected values of Zdr under certain weather conditions such as light precipitation.

Now that the network upgrade is essentially complete, and the ROC has implemented monitoring processes, it has become evident that the calibration process is not producing consistent results. The ROC team has observed that up to 40% of the sites have estimated system bias errors of greater than 0.2 dB (Cunningham, 2013). This observation is based on the use of the weather comparison method mentioned above as well as a new method based on the use of the daily sun spikes seen each morning and evening (Holleman, 2010). In addition to these methods, the ROC is developing another external target method based on Bragg scatter ((Melnikov, 2013). This latter method is based on the assumption that the Bragg scatter is also polarization neutral like the solar radiation noise power.

This level of error, estimated by these methods, can affect the polarimetric Quantitative Precipitation Estimator (QPE), lowering rain rate estimate accuracy. For errors in the 0.3 to 0.4 dB range, the accuracy approaches that of the non-polarimetric estimators. However, substantial benefits are achieved in hydrometeor classification and identification of warning indicators such as Zdr columns and debris signatures.

The ROC hotline provides assistance to sites that may be incorrectly calibrated. The ROC can become involved when the operational community observes issues with Zdr estimates or precipitation estimator outputs. The ROC also monitors performance of the sites and can offer assistance when unusually poor performance is noted.

The engineering teams also can monitor the statistics of the three critical calibration parameters. This data may prove useful for improving technical manual procedures and test equipment in the field. Figure 8 is a histogram of the reflector bias adaptable parameter from 146 sites as of March 2013. While the majority of the

sites reported reflector bias values of near zero, there are many that have unexpectedly large bias values. Errors in the reflector bias can exacerbate problems with overall system calibration because this bias is counted twice in the calibration correction equations because it enters into both the transmit and receive components of the Zdr estimate.

Figures 9 and 10 show similar histograms for the power sense and test signal bias for the same 146 sites. The ROC team plans to continue investigating the field performance and the effects the variance of these parameters has on the calibration accuracy.

While the ROC teams are developing external verification methods through the use of weather signals and the sun, they have also been implementing and testing an alternate method based on measuring the power returned from ground clutter in the cross polarization receiver channels. The next section provides a description and status of this independent method.

5. CROSS POLARIZATION POWER

The National Center for Atmospheric Research (NCAR) developed an external calibration method for use on the S-pol radar that utilizes ground clutter and solar scans. The unique feature of this method is that the ground clutter scans are based on the cross polarization scatter components, or the off diagonal terms of the radar scattering matrix. This method takes advantage of the radar reciprocity principle that states that the cross polarization powers returned from either precipitation or clutter targets (i.e. transmit H, receive V – transmit V, receive H) are equal assuming that the transmitted powers are equal (Hubbert, 2003). See Figure 11 for a simple demonstration of the concept based on use of ground clutter for the targets.

Along with the clutter (or precipitation) cross polarization power scans, this method requires a solar scan. By combining the power ratios and the solar scan outputs, the system bias can be obtained as shown in the equation below adapted from Hubbert, 2003.

$$Zdr_{true} = Zdr_{meas} * \frac{CP_{xv}}{CP_{xh}} * (Sun)^2$$

In this equation, "Sun" is the mean ratio of the V channel to the H channel noise powers observed during a scan of the solar disk.

See Figure 12 for the terms needed to describe a simple proof of the cross polarization method. In Figure 12, all the relevant terms for comparing the intrinsic (or true) value for Zdr to the measured Zdr are indicated. These include all the hardware gains and losses and transmitter powers. This figure shows the origin of key parameters in the measured Zdr and the cross polar powers of the equation above.

Figure 13 is the algebraic demonstration of how the sun ratio and the cross polar power ratios combine to form the system bias. The "key to success" for this proof is that the sun ratio is defined as vertical noise to horizontal noise power, the inverse of convention. This key element results in almost all of the terms in the Zdr_{true} equation to cancel out. The sun noise power ratios are assumed to be unity (the sun does not exhibit a polarization preference at microwave frequencies), and the cross polarization clutter power ratio is assumed to equal one via reciprocity.

The validity of the cross polarization power method has been extensively verified on the S-pol radar (Hubbert, 2007, 2011). NCAR first developed and verified the method using precipitation while operating the S-pol radar in the so called "fast alternating" mode which uses a high speed rotary waveguide switch to alternately transmit the H and V pulses. This allowed the cross polar power pairs (CP_{XV}/CP_{XH}) to be obtained close together in time sequence. The NCAR team conducted vertical pointing calibrations in conjunction with the cross polarization power measurements and verified that the accuracies of the two methods are equivalent.

For application to the WSR-88D, NCAR modified the original cross pol methods and collected data in the so-called "PPI Mode". This approach used alternating 360 degree scans, first one polarization, say H, followed by another scan using the alternate (or V) polarization. This meant that the H and V cross pol returns were not obtained closely in time. However, NCAR found that on the S-pol radar, the results were still sufficient to conclude that cross pol could yield the system Zdr bias values equivalent to the vertical pointing method.

Based on NCAR's results on S-pol, the ROC began implementation of the cross polarization power method on the WSR-88D. ROC software engineers modified the sun scan utility to generate the NCAR designed box scans and added utility code to control the radar in order to collect the sequential single polarization clutter powers. The following section describes the

results from collecting cross polarization data on the test bed radars in Norman OK (KCRI and KOUN).

6. CHALLENGES TO IMPLEMENTATION OF CROSS POLARIZATION POWER

In the course of implementing and testing the WSR-88D version of cross polarization power, the ROC and NCAR teams met several significant challenges. These challenges related to the cross polarization clutter power ratios, the solar scan derived reflector bias, and the transmitter power monitoring.

6.1 Clutter Power Ratio Challenges

The first observation from the cross polar power calibration data collected on KCRI was that the component of the system bias derived from the clutter ratios depended on azimuth. Figure 14 shows the average clutter power ratios as a function of azimuth. While a mean value may be inferred from the plot (approximately 0.85), the variance is too large for this to meet the overall accuracy requirement of 0.1 dB. ROC engineers spend considerable effort in tracking down the source of this variation. Possible contributions from the radome, ground clutter, and sidelobes were considered and dismissed. The source was finally tracked to the pedestal elevation control.

As the pedestal was scanning through 360 degrees, the control mechanism was not maintaining the elevation at the commanded angle. Periodic changes in elevation, excursions about the commanded angle, were occurring. This is because of imbalances in the antenna caused it to drift away from the commanded elevation. The control system did not generate a correction until the drift exceeded the precision of the optical encoders. For the WSR-88D, the precision of the encoders is 0.04 degrees. Then the control would drive the elevation motors to correct the drift. This resulted in a periodic oscillation about the commanded elevation. See Figure 15, which shows the likelihood that one of these elevation corrections may occur at a particular azimuth. This plot was derived from the same data set used in Figure 14. There are seven oscillations in the data for both figures, indicating that the variance in the clutter power ratios is caused by the elevation instability.

The fact that the pedestal does not reliably maintain the commanded elevation angle leads to an issue with a basic assumption of the cross polarization power theory. That is the assumption of radar reciprocity. For reciprocity to hold, the cross polarization power ratio must be derived from common clutter resolution volumes. The sequential H and V clutter powers must come from the same patches of clutter. With the observed variations in elevation control, this was not the case most of the time. After an H only scan, the following V only scan resolution volumes were not matching. This is the source of the large variance in the ratios. It also explains observed differences in WSR-88D and S-pol data from previous experiments.

Figure 16 (Hubbert, 2011) illustrates the problem. The scatter plots of the cross pol clutter power ratios for KOUN and S-pol exhibit a striking difference, with the KOUN data having much larger variance. At the time, Hubbert concluded that the large variance was due to isolation issues in the variable phase power divider. However it is much more likely the variance was due to the antenna pedestal control instability.

The S-pol antenna features a much more precise positioning mechanism. As it turns out, the pointing precision of S-pol is about 0.005, an order of magnitude better than the WSR-88D.

The ROC team dealt with this new problem by redesigning the scan process. Initially the software started each scan at random locations, basically keeping the antenna scanning while reconfiguring the power divider and conducing noise power, transmitter power measurements, and receiver bias checks. This exacerbated the instability problems and increasing the probability that subsequent scans would not revisit the same clutter resolution volumes. Engineers changed the scan design so that the H and V scans would always have the same initial conditions by returning the antenna to a known position prior to initiating a clutter scan. This helped to reduce the variances.

The ROC and NCAR teams encountered another unexpected problem while examining the behavior of the cross polar power ratios (VH/HV). See Figure 17, which is a plot of these ratios displayed by radial and range. The colors represent the ratio, which by reciprocity, should have a mean of near zero, biased only by the radar hardware. While many of the values appear to be between -10 and +10 dB (yellow and green colors), there are certain ranges where the ratio is quite larger, as seen in the red and blue steaks. Engineers have yet to determine the cause of these unexpected data points.

The teams also explored alternate methods, including stopping the antenna at each of the indexed azimuths and even locking the antenna in the two available azimuth stow positions. None of these method reduced the variance significantly and were not employed. The locked pedestal experiment did not yield enough data

points from the two azimuths and was deemed impractical for field implementation anyway.

The most recent design of the cross polarization data collection, including the solar scans, is presented below to show the complexity of the approach necessary to deal with the pedestal control performance:

For each cycle:
  If the sun is in range, run a sunscan:
    transmitter on, PRF code 5 (~1000Hz)
  Run receiver bias (Transmitter off)
  Do 3 cycles of:
    Park the pedestal
    Transmitter on, PRF code 5
    Put the divider to H "Only"
    Run power sense (H-only)
    Run receiver bias (Transmitter off)
    Transmitter on, PRF code 5
    Do H Clutter Scan
    Park the pedestal
    Put the divider to V "Only"
    Do V Clutter Scan
    Park the pedestal
    Run power sense (V-only)
    (The rest of this just repeats the above with H & V swapped)
    Park the pedestal
    Put the divider to V "Only"
    Run power sense (V-only)
    Run receiver bias (Transmitter off)
    Transmitter on, PRF code 5
    Do V Clutter Scan
    Park the pedestal
    Put the divider to H "Only"
    Do H Clutter Scan
    Park the pedestal
    Run power sense (H-only)
  Put the divider to Balanced
  Run power sense

This process is repeated enough times to collect large data sets in order to reduce the variance. Figure 18 is a sample of the cross pol clutter ratios scatter derived from the improved strategy.

While the ROC was developing the scan designs to deal with the pedestal control issues, NCAR developed sophisticated data sorting and filtering methods. These methods are aimed at eliminating H and V clutter power ratios that may have been derived from non-matching clutter resolution volumes. Meymaris, 2013, presents details of the cross polarization implementation on the WSR-88D.

One set of filter criteria used by NCAR is presented below to illustrate the approach. These filters are under constant study and review and do not necessarily represent the final values.

Hcpa_co between .5 and .995
Vcpa_co between .5 and .995
abs(Hcpa_co-Vcpa_co)<.4
(Hsnr_cross+Vsnr_cross)/2 between 10 and 70
abs(Zdr_copolar)<4
(Hldr+Vldr)/2 between -25 and -5
(Hsnr_co+Vsnr_co)/2 between 30 and 70

Hcpa and Vcpa are the horizontal and vertical return Clutter Phase Alignments, a coherency parameter used in the Clutter Mitigation Decision (CMD) algorithm implemented in the WSR-88D (Ice, 2009). Hldr and Vldr refer to linear depolarization ratio.

The combination of the data sorting and filtering and careful design of the scan strategy has been reducing the variance of the cross polar power ratios. The filtering, especially use of the LDR variable, has also been useful in eliminating the unexplained large cross polar power ratios seen in Figure 17. Figure 19 shows 24 hours of data that includes the clutter power ratios, the solar scan data, and receiver bias data. The overall variance of the power ratios are about 0.044.

6.2 Antenna Bias Measurement Challenges

The second key component of the cross polarization power derived system bias is the “sun” measurement component. The ROC and NCAR teams have analyzed the sun source derived reflector bias and have observed a diurnal variation. Figure 20 shows five days of solar scan derived bias data obtained in December 2012 from the KOUN radar. A distinct daily variation nearly 0.1 dB is seen in the plots.

The teams currently have no explanation for this variation. The lower right inset of Figure 20 is a scatterplot of the bias vs. radome temperature and shows a weak correlation. Perhaps the antenna structure itself exhibits thermal expansion sufficient to change the reflector bias over a daily cycle. The teams have also speculated that the time of day, with the corresponding sun elevation angles, may play a role. This may be the case if the angle of the solar microwave signal propagating through the atmosphere somehow affects the polarization state.

If the antenna truly does exhibit a variance in bias over temperature, this can be a significant challenge for maintaining accurate Zdr calibration. This is an area for future investigation and research.

6.3 Transmitter Power Monitoring Challenges

The transmitter power splitting function is different for S-pol and the WSR-88D. The S-pol

radar features a divider, waveguide switches, and dummy loads configured so that the H only and V only transmitted power levels are identical to the powers transmitted during the simultaneous transmission operational mode. This means that the powers do not need to be monitored for the cross polarization data collections.

The WSR-88D employs a variable phase power divider, which has to be set to generate all H or V power for the clutter scans. Then the normal setting is for a 50/50 split. So the operational powers are approximately half of the powers used in the cross polarization power scans. This means that the ratio of the "full" powers to the "half" powers for both channels must be measured. Then a correction factor is added to the cross polarization system bias equation (Hubbert, 2011).

Fortunately the ratios in question are for each mode separately, that is the half H to full H and half V to full V ratios. This means that errors in the power sense bias calibration do not affect these ratios as the powers are measured through the same hardware paths in the BITE.

The ROC and NCAR analyzed the transmitter power monitoring data and have noted a potential issue. The transmitter powers are not fully stable for significant periods of time after the reconfiguration of the variable phase power dividers. Figure 21 shows how the measured power changes during the scan cycles, with the largest variations occurring after the sun scan portions of the collection process.

The ROC and NCAR are currently analyzing this behavior and will modify the collection approach as needed to reduce error contributions from transmitter power monitoring.

7. THE LESSONS

The overall performance of the polarimetric WSR-88D with respect to Zdr calibration is steadily improving through the efforts underway at the ROC. Sites that are having issues with calibration can be identified and assisted as needed through use of network wide monitoring tools becoming available. The use of the daily sunspike and emerging capabilities based on Bragg scatter as an external target show real promise in establishing and maintaining good Zdr calibration.

The state of calibration for Zdr is more mature at this point of deployment than reflectivity calibration was at a similar juncture in the early days of NEXRAD. Given the challenges summarized here, the fact that 54 to 58% of the network sites are believed to be well calibrated is noteworthy. Most of the network radars have been polarimetric for less than a year. The ROC continues to work with the field to identify and correct issues. The ROC science and engineering teams, supported by NCAR and NSSL, continue to develop tools for monitoring network performance.

Cross polar power continues to be a potential for a true external calibration technique that could rival the vertical pointing method. This will be the case if the ROC and NCAR teams can surmount the challenges presented by the WSR-88D implementation. The serious challenges to date derive from major differences in the hardware design of the S-pol radar, where the cross pol method was developed, and the WSR-88D. The major differences are in the pedestal control and transmit power division. Some other differences which could account for the performance challenge are the antenna design and the location of the low noise amplifiers.

The S-pol radar features a robustly designed antenna that is not enclosed in a radome. The S-pol antenna is much more mechanically rigid than the WSR-88D, which is housed in a radome. The radome itself may be contributing to the observed performance issues. The S-pol low noise amplifiers are located in a climate controlled shelter while the WSR-88D amplifiers are in the RF Pallet, housed in the radome. However, the WSR-88D amplifiers are provided with internal temperature compensation. It remains to be seen if the temperature performance differences are an issue, perhaps affecting receiver linearity. There are some early indications that there is a slight mismatch in linearity between the H and V receivers in the WSR-88D that could affect Zdr accuracy (Melnikov, 2013).

All of these items highlight the challenges of migrating research capabilities into operational radar networks. What works well in a research environment may not be easily adapted to production systems. When planning new field capabilities based on scientific research, engineers need to be cognizant of the differences between research platforms and the target field systems. This can be dealt with through careful planning for all Research to Operations (R2O) processes. The lessons learned in this project and other recent enhancements are being applied to future work.

ACKNOWLEDGEMENTS

The authors wish to express appreciation to John Hubbert, Greg Meymaris and Mike Dixon of NCAR for their technical support to the cross

polarization power calibration project, and to Valery Melnikov of NSSL for his excellent analysis of the current calibration methods.

REFERENCES

Balaji, M. S., J. R. Ellis, W. H. Walker, D. R. Cartwright, J. H. Lee, J. H. Romines, 2012, An Engineering Illustration of the Dual Polarization upgrade for the WSR-88D, ERAD 2012, *7th European Conference on Radar in Meteorology and Hydrology.*

Berkowitz, D. S., J. A. Schultz, S. Vasiloff, K. L. Elmore, C. D. Payne, and J. B. Boettcher, 2013, Status of Dual Pol QPE in the WSR-88D Network, *27th Conference on Hydrology.*

Baron Services, 2011, ZDR Calibration Accuracy Analysis, BS-2000-000-107, Available from Baron Services Inc. 4930 Research Dr., Huntsville Alabama, 35805 USA

Cunningham, J. G., W. D. Zittel, R. R. Lee and R. L. Ice, 2013, Methods for Identifying Systematic Differential Reflectivity (Zdr) Biases on the Operational WSR-88D Network, *36th Conference on Radar Meteorology.*

Gorgucci, E, S. Gianfranco, and V. Chandrasekar, 1999, A Procedure to Calibrate Multiparameter Weather Radar Using Properties of the Rain Medium, *IEEE Trans. On Geoscience and Remote Sensing*, Vol. 37, No 1, Jan 1999.

Gourley, J. J., B. Kaney, and R. A. Maddox, 2003, Evaluating the Calibrations of Radars: A Software Approach, *31st Conference on Radar Meteorology.*

Holleman, I, A. Huuskonen, R. Gill, P. Tabary, 2010: Operational monitoring of radar differential reflectivity using the sun. *J. Atmos Oceanic Technol.,* **27**, 881-887.

Hubbert, J. C., V. N. Bringi, and D. Brunkow, 2003, Studies of the Polarimetric Covariance Matrix. Part I: Calibration Methodology, *J. Atmos. Oceanic Technol.*, **20**, 696 - 706.

Hubbert, J. C., F. Pratte, M. Dixon, R. Rilling, and S. Ellis, 2007, Calibration of Zdr for NEXRAD, *23rd International Conference on Interactive Information Processing Systems for Meteorology, Oceanography, and Hydrology.*

Hubbert, J. C., Dixon, M., Chandrasekar, V.,Brunkow, D. A., Kennedy, P. C., Ice, R. L., and Saxion, D., 2011, Zdr Calibration and Simultaneous Horizontal and Vertical Polarization Transmit Radars, *35th Conference on Radar Meteorology.*

Ice, R. L., D. A. Warde, F. Pratte, 2005, Investigating External and Dual Polarization Calibration Options for the WSR-88D, *32nd Conference on Radar Meteorology.*

Ice, R. L., R. D. Rhoton, J. C. Krause, D. S. Saxion, O. E. Boydstun, A. K. Heck, J. N. Chrisman, D. S. Berkowitz, W. D. Zittel, and D. A. Warde, 2009, Automatic Clutter Mitigation in the WSR-88D, Design, Evaluation, and Implementation, *34th Conference on Radar Meteorology.*

Melnikov, V. and D. Zrnic, 2013, Calibrating Differential Reflectivity in the WSR-88D, Internal Report, National Severe Storms Laboratory.

Meymaris, G, J. C. Hubbert, M. Dixon, R. L. Ice, A. K. Heck, and J. G. Cunningham, 2013, Operational considerations for Zdr Calibration using the Cross-polarimetric Technique, *36th Conference on Radar Meteorology.*

Ryzhkov, A. V. et al, 2005, Calibration Issues of Dual-Polarization Radar Measurements, *J. Atmos. Oceanic Technol.*, **22**, 1138 - 1155.

Saxion, D. S. and R. L. Ice, New Science for the WSR-88D: Status of the Dual Polarization Upgrade, 2012, *28th International Conference on Interactive Information Processing Systems for Meteorology, Oceanography, and Hydrology.*

Sirmans, D., 1992, Calibration of the WSR-88D, Operational Support Facility Report, Available from the WSR-88D Radar Operations Center.

Smith, P. L, The Unit Symbol for the Logarithmic Scale of Radar Reflectivity Factors, 2010, *J. Atmos. Oceanic Technol.*, **27**, 615 – 616.

Zrnic, D. S., Melnikov, V. M. and J. K. Carter, 2006, Calibrating Differential Reflectivity on the WSR-88D, *J. Atmos. Oceanic Technol.*, **23**, 944 - 951.

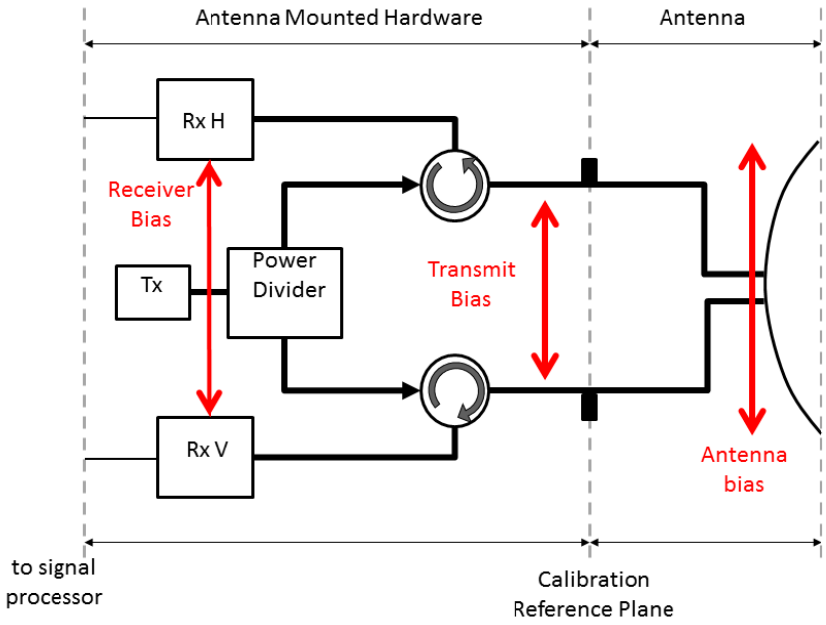

Figure 1 – Calibration Subsystems Block Diagram

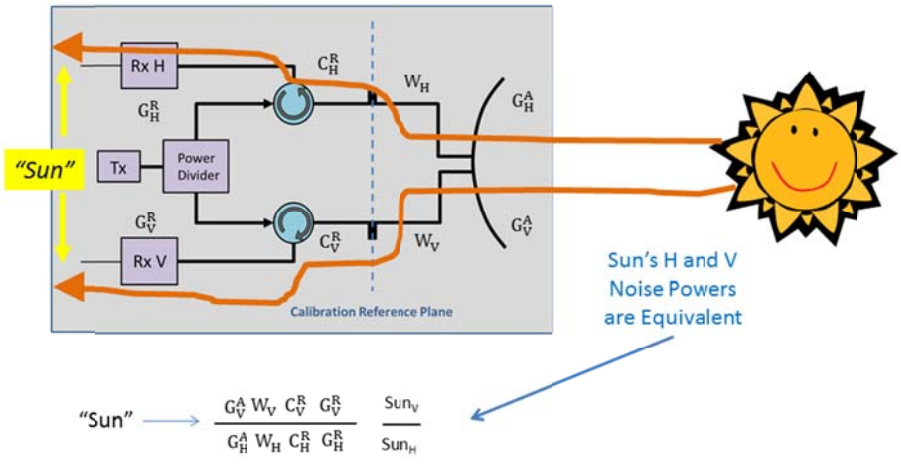

Figure 2 – Solar Scan to Obtain Antenna Bias

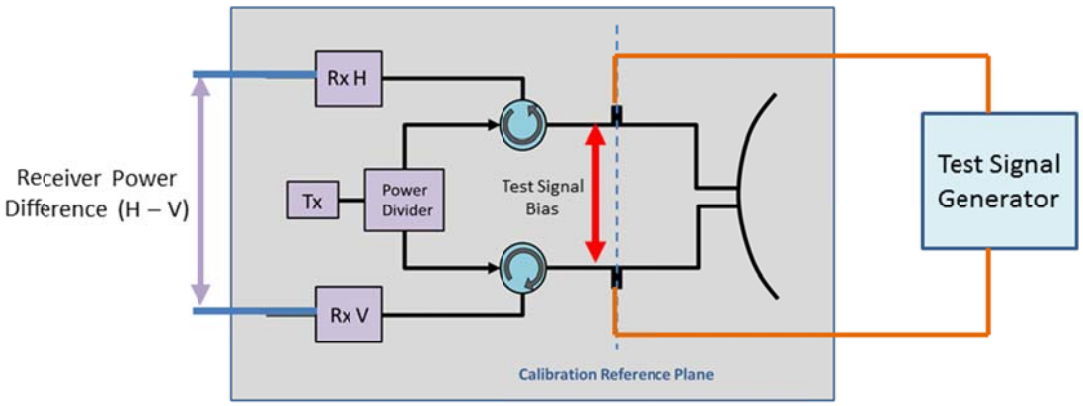

Figure 3 – Receiver Bias Measurement

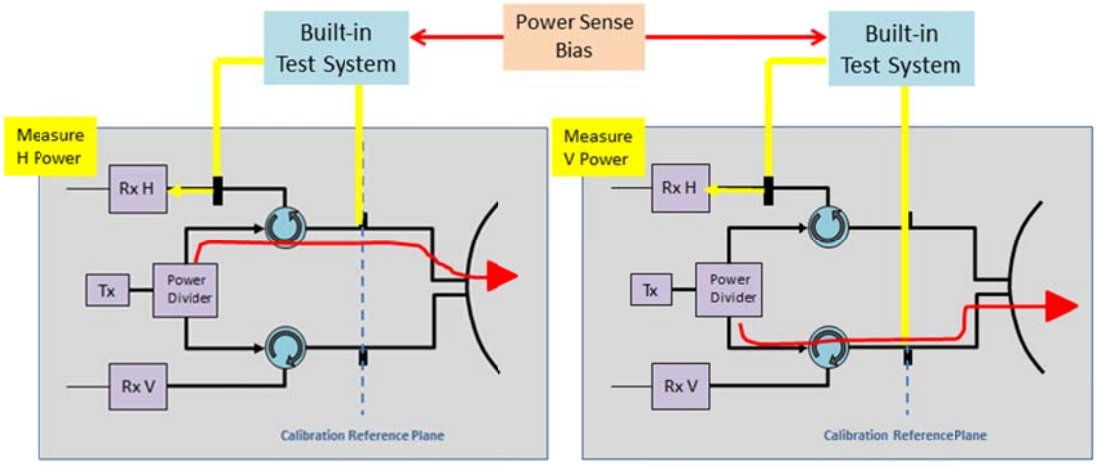

Figure 4 – Transmitter Power Measurement

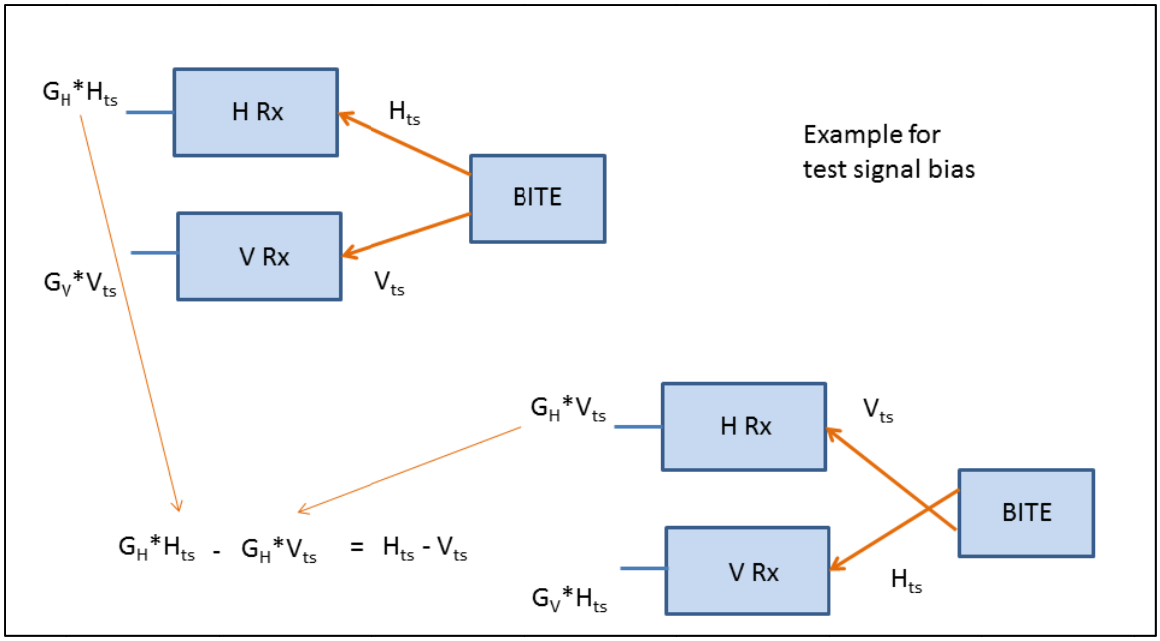

Figure 5 – Test Signal Bias Measurement

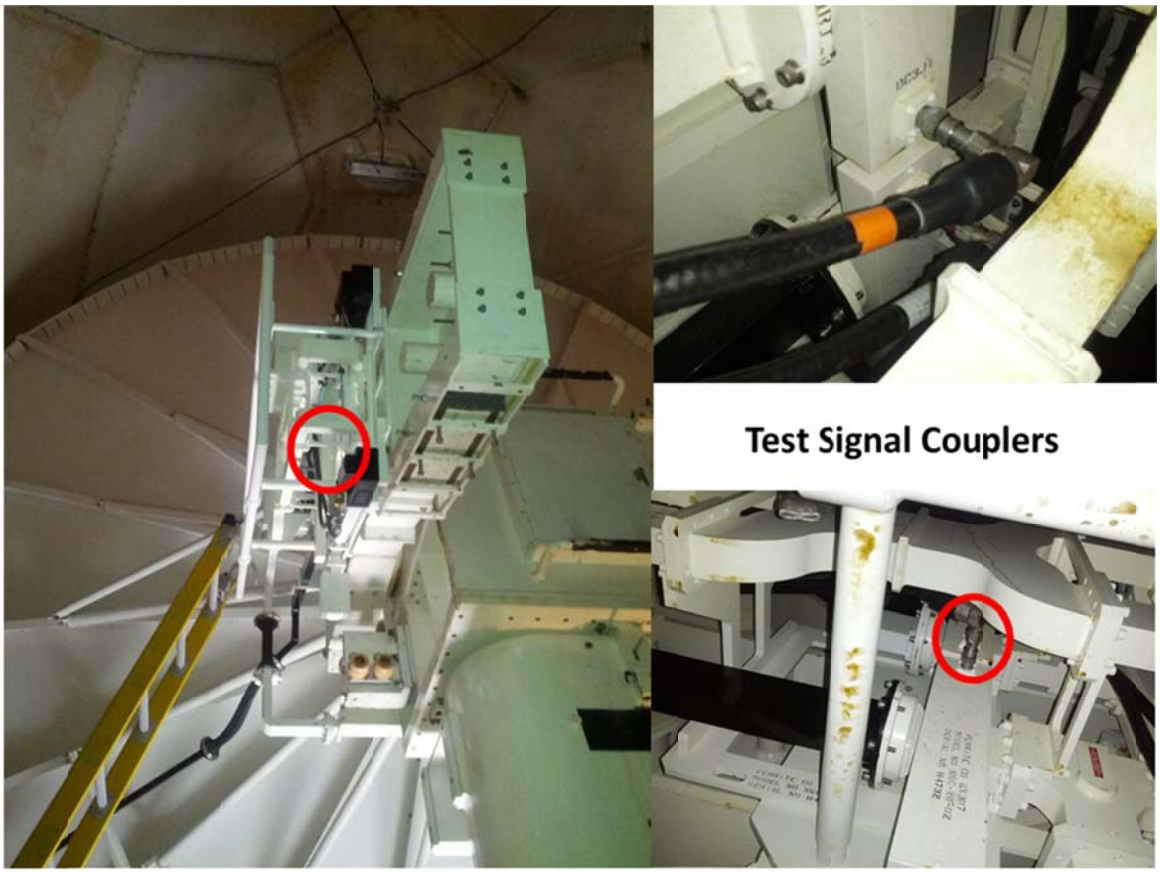

Figure 6 – RF Pallet, Ladder, and Test Signal Couplers

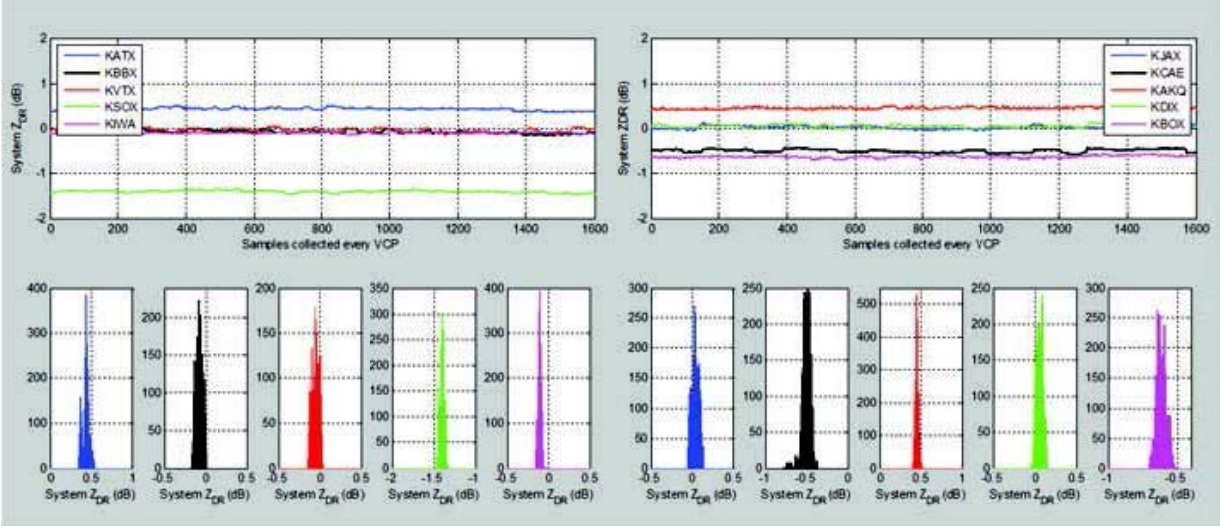

Figure 7 – System ZDR from Ten Early WSR-88D Upgrade Sites (Balaji 2012)

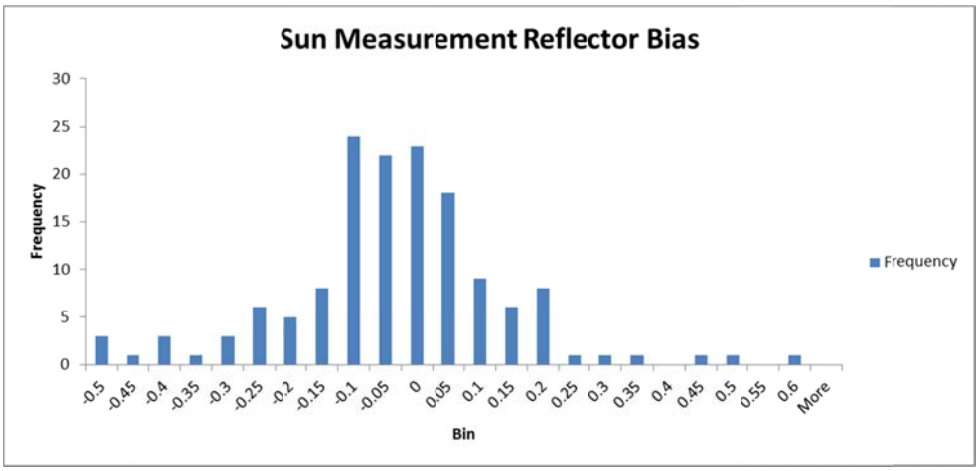

Figure 8 – Reflector Bias for 146 Sites

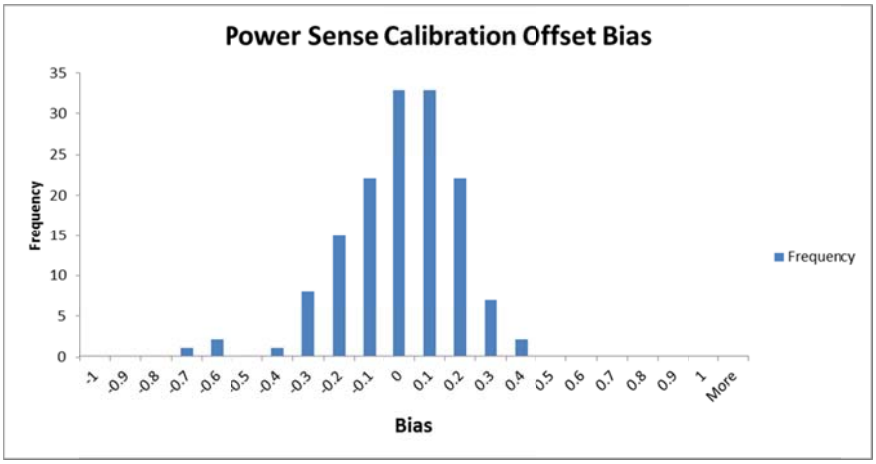

Figure 9 – Power Sense Bias for 146 Sites

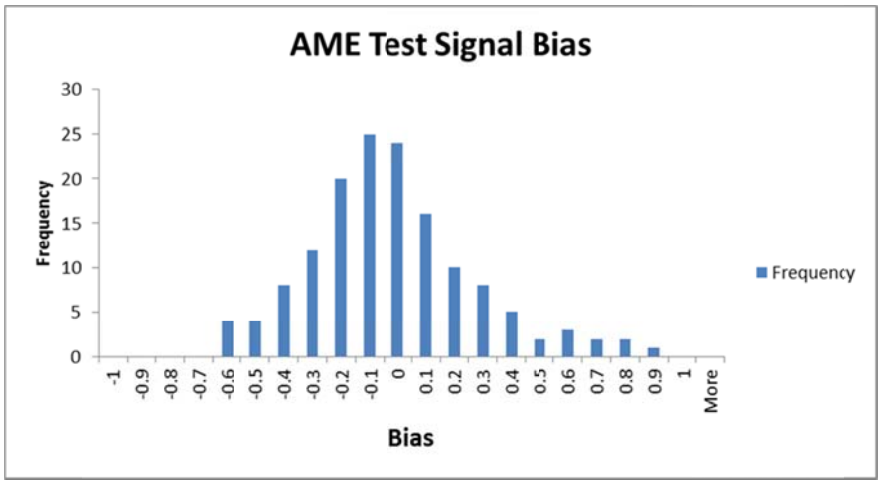

Figure 10 – Test Signal Bias for 146 Sites

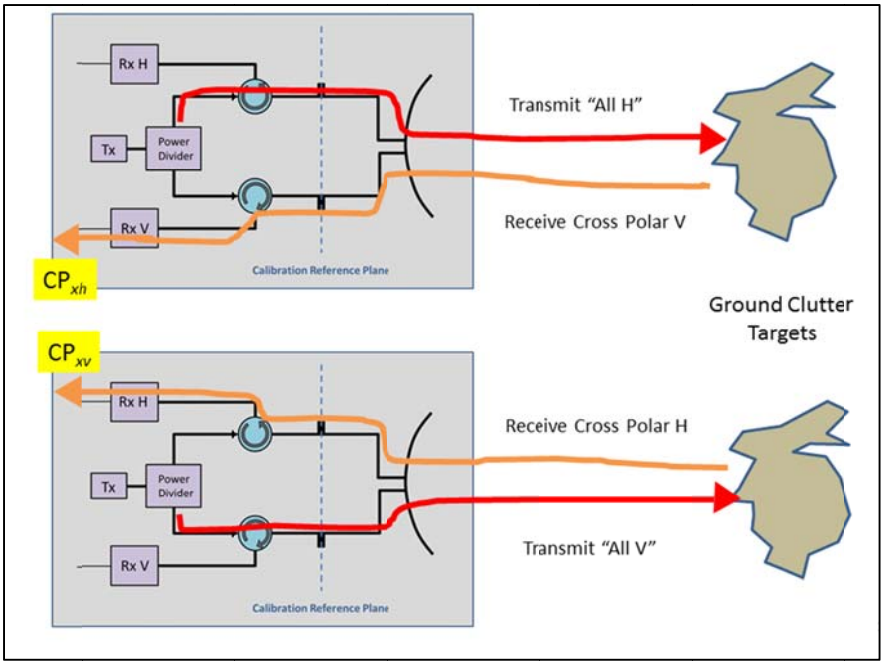

Figure 11 – Cross Polarization Clutter Power Ratio Measurement

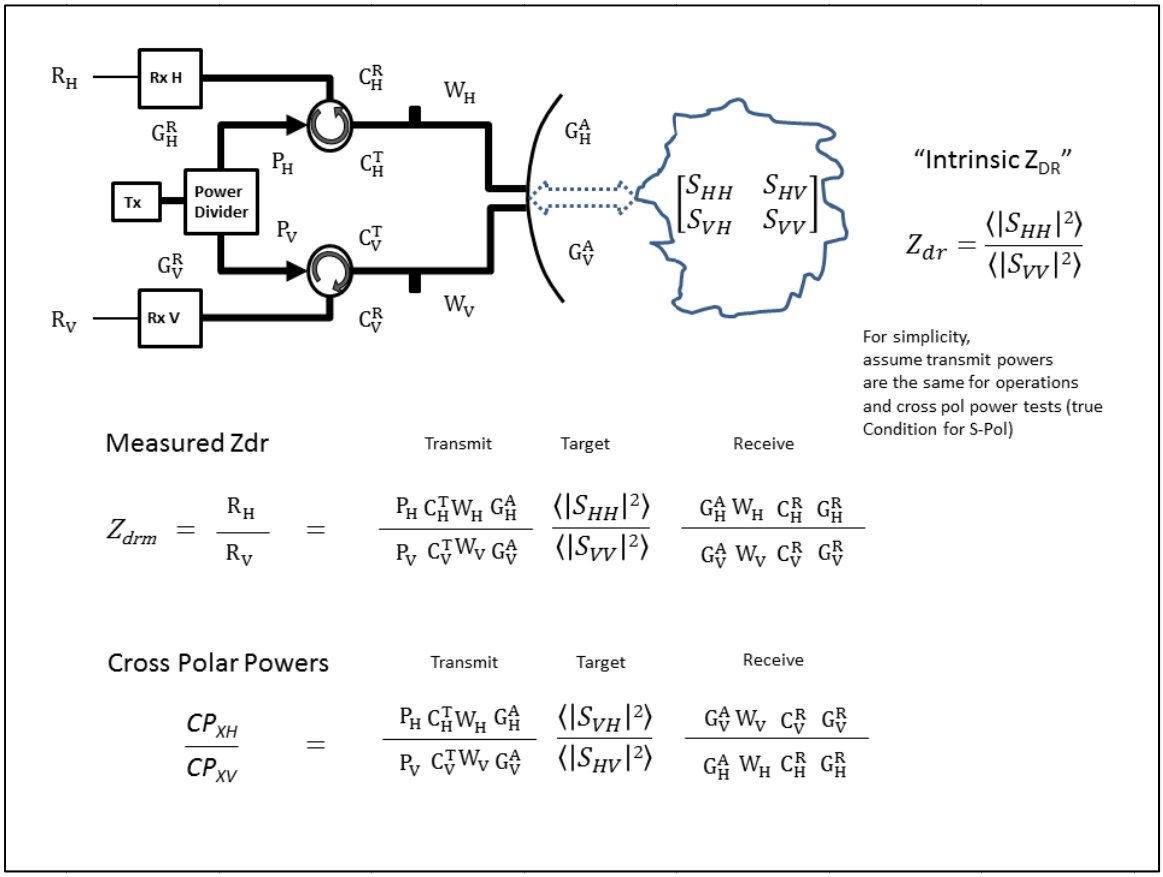

Figure 12 – Cross Polarization Power Relevant Terms

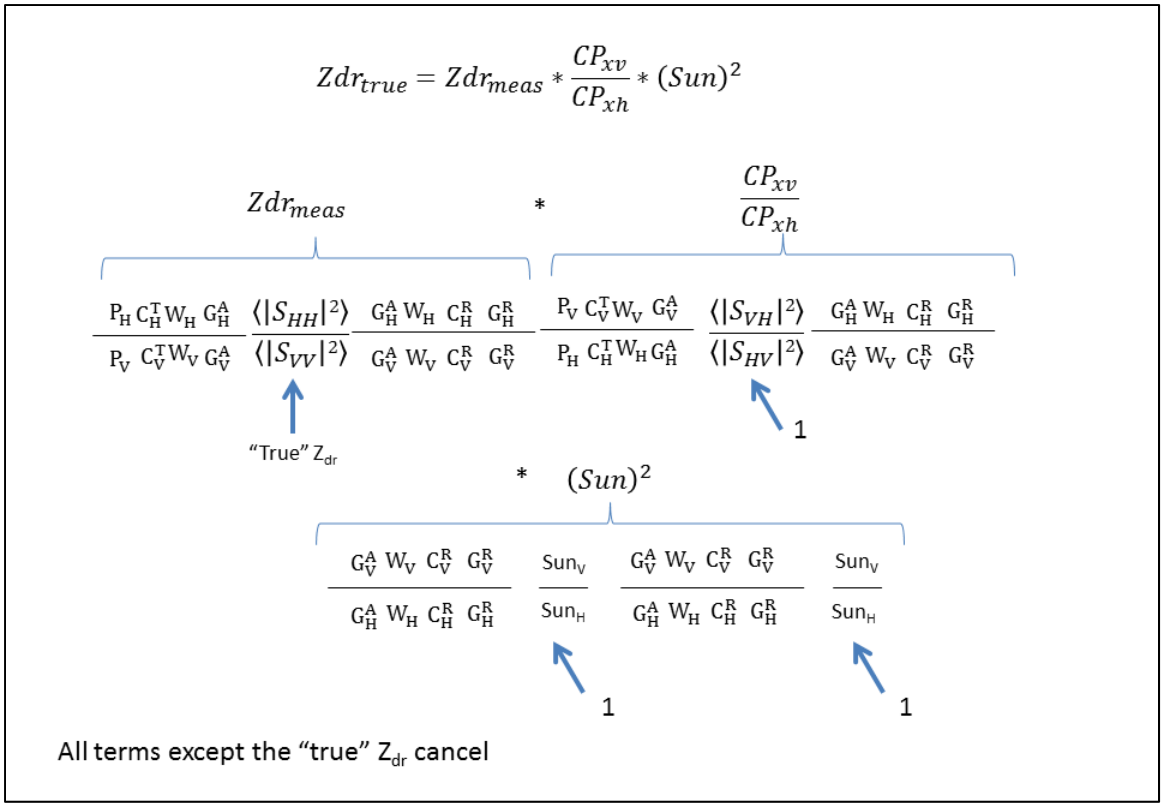

Figure 13 – Algebra Demonstration of Cross Polarization Power

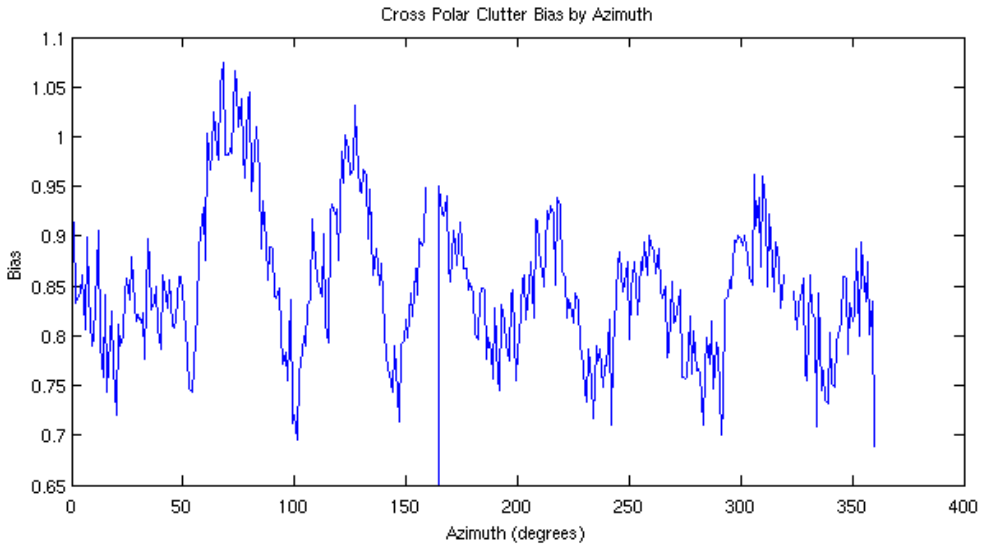

Figure 14 - Clutter Power Ratio Component of Cross Polarizaiton Power Derived Bias – By Azimuth

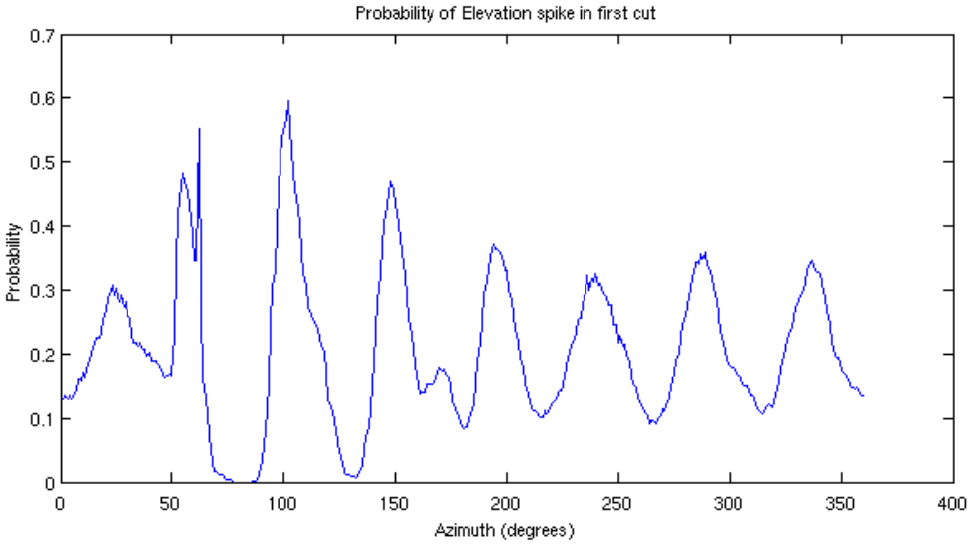

Figure 15 – Probability of an Elevation Angle Change by Azimuth

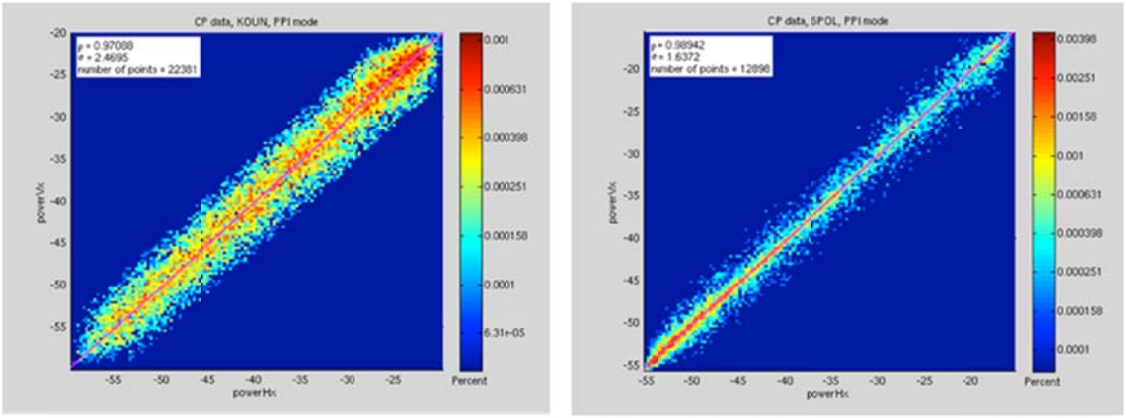

Figure 16 – Cross Pol Clutter Ratios Scatterplots - KOUN (left) S-pol (Right) (Source: NCAR)

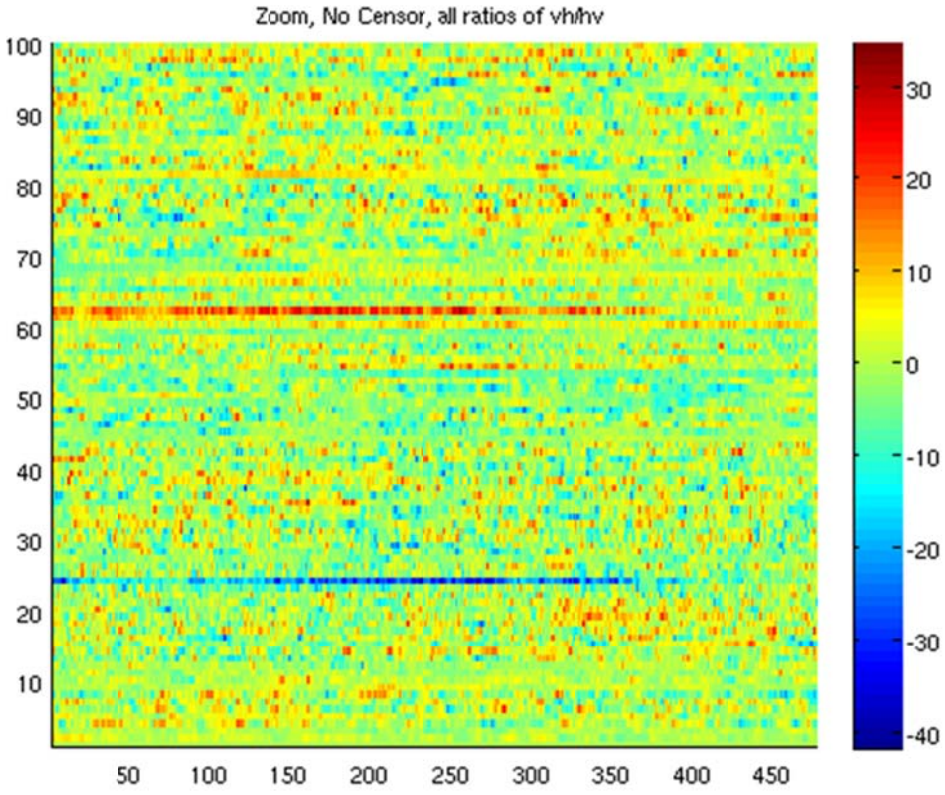

Figure 17, Range –Azimuth Plot of VH/HV

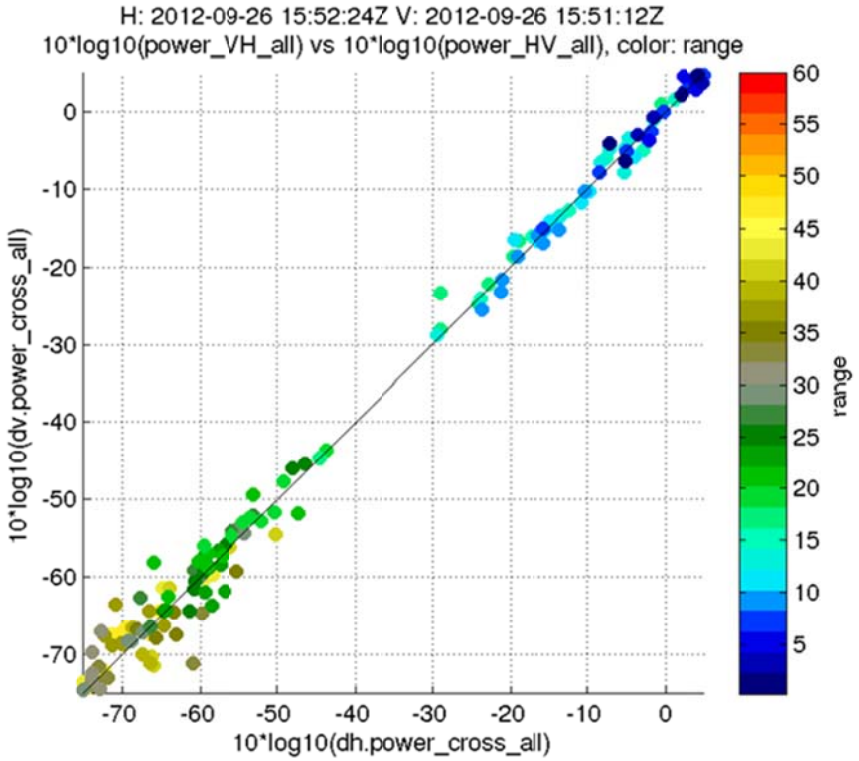

Figure 18 – Scatterplot of Cross Pol Clutter Power Ratios – KOUN (Source: NCAR)

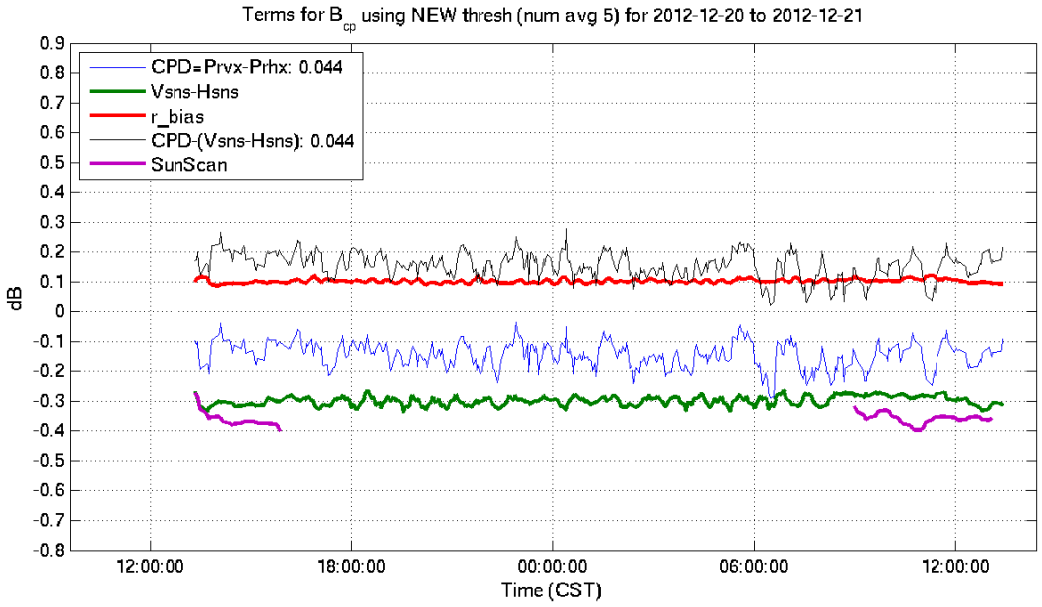

Figure 19 – Clutter Power Ratios with Data Sorting Filters Applied (Source: NCAR)

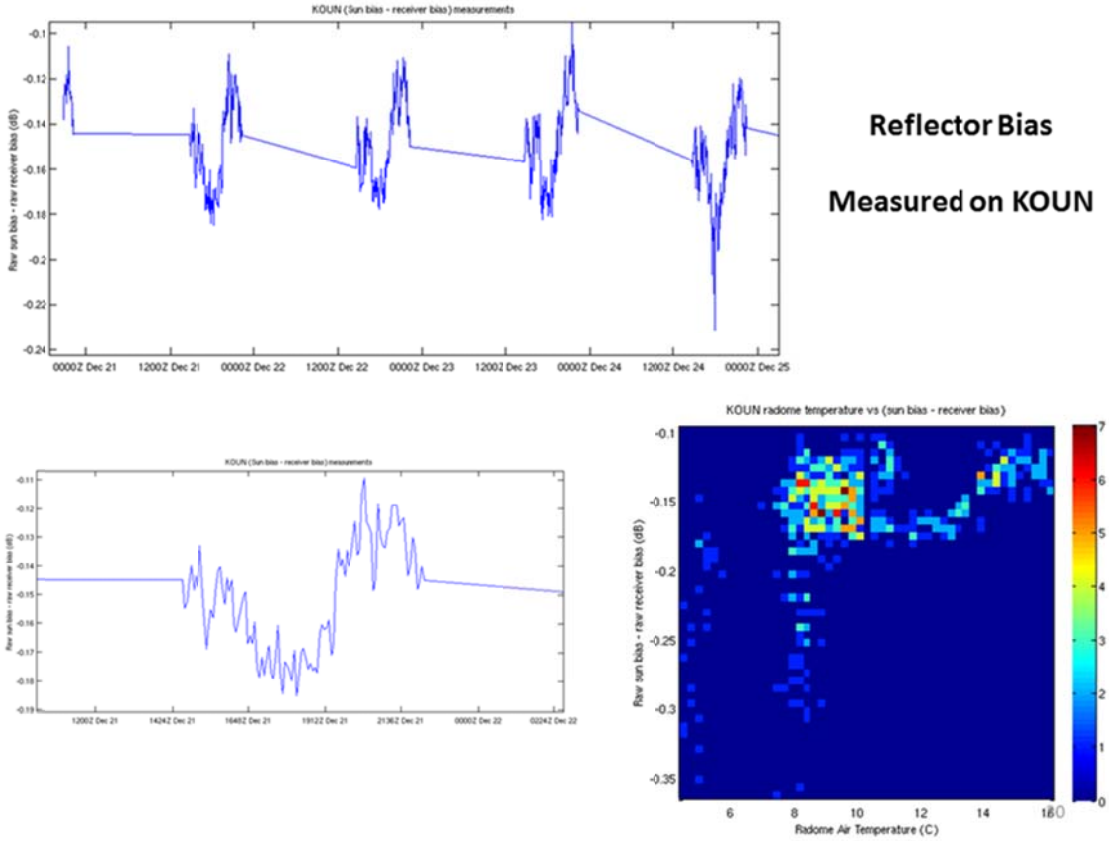

Figure 20 – Reflector Bias Diurnal Variation Observed

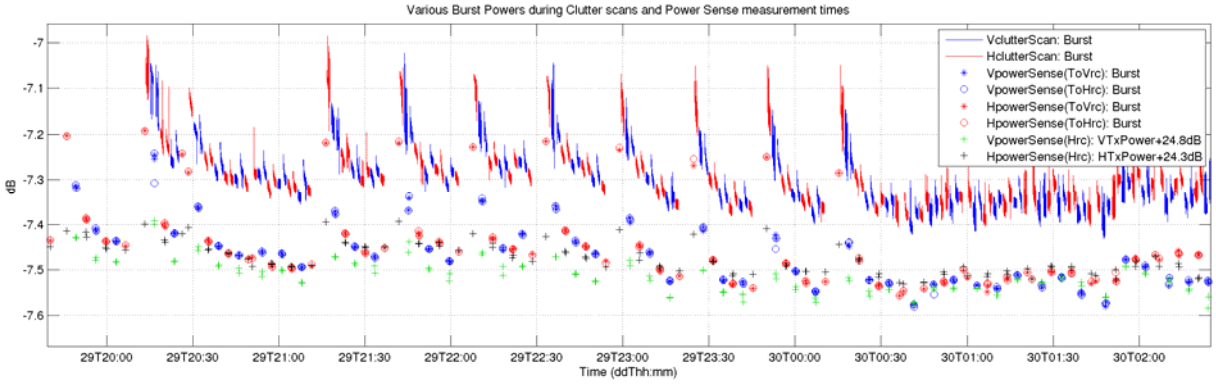

Figure 21 – Transmitter Power Stability Analysis (Source: NCAR)